Acta Cryst E CRYSTALLOGRAPHIC COMMUNICATIONS

ISSN 2056-9890

Crystal structure, Hirshfeld surface analysis and DFT calculations of ethyl 2-[4-(methylsulfanyl)-1*H*-pyrazolo[3,4-*d*]pyrimidin-1-yl]acetate

Younesse Ait Elmachkouri,[a] Ezaddine Irrou,[a] Samira Dalbouha,[b,c] Hassan Ouachtak,[a] Joel T. Mague,[d] Tuncer Hökelek,[e] Lhoussaine El Ghayati,[f] Nada Kheira Sebbar[a,f]* and Mohamed Labd Taha[a]

[a]Laboratory of Organic and Physical Chemistry, Applied Bioorganic Chemistry Team, Faculty of Sciences, Ibn Zohr University, Agadir, Morocco, [b]Laboratory of Organic Chemistry and Physical Chemistry, Research Team: Molecular, Modeling, Materials and Environment, Department of Chemistry, Faculty of, Sciences, University Ibn Zohr in Agadir, BP 8106 Agadir, Morocco, [c]Laboratory of Spectroscopy, Molecular Modeling, Materials, Nanomaterials, Water, and Environment, CERNE2D, Faculty of Sciences, Mohammed V University in Rabat, Av. Ibn Battouta, BP 1014, Rabat, Morocco, [d]Department of Chemistry, Tulane University, New Orleans, LA 70118, USA, [e]Department of Physics, Hacettepe University, 06800 Beytepe, Ankara, Türkiye, and [f]Laboratory of Heterocyclic Organic Chemistry, Medicines Science Research Center, Pharmacochemistry Competence Center, Mohammed V University in Rabat, Faculty of Sciences, Morocco. *Correspondence e-mail: n.sebbar@uiz.ac.ma

Received 10 October 2022
Accepted 20 November 2022

Edited by M. Weil, Vienna University of Technology, Austria

Keywords: crystal structure; hydrogen bond; π-stacking; pyrazolopyrimidine.

CCDC reference: 2221106

Supporting information: this article has supporting information at journals.iucr.org/e

The asymmetric unit of the title compound, $C_{10}H_{12}N_4O_2S$, contains two molecules differing slightly in the orientations of the methyl groups. In the crystal, a sandwich-type structure extending parallel to the *ab* plane is formed by weak C—H···O and C—H···N hydrogen bonds together with slipped π-stacking interactions. A Hirshfeld surface analysis of the crystal structure indicates that the most important contributions to the crystal packing are from H···H (43.5%), H···O/O···H (17.9%) and H···N/N···H (17.4%) interactions. The molecular structure optimized by density functional theory (DFT) at the B3LYP/ 6–311 G(d,p) level is compared with the experimentally determined structure in the solid state. Further calculations include the HOMO–LUMO energies and molecular electrostatic potential (MEP) surfaces.

1. Chemical context

Pyrazolo[3,4-*d*]pyrimidine derivatives are an important class of nitrogen-containing compounds because of their pharmacological properties and their use as antitumor agents (Tintori *et al.*, 2015). They are also applied as protein kinase inhibitors (Schenone *et al.*, 2014; Rao & Chanda, 2020), and have anti-HSV (Moukha-Chafiq *et al.*, 2007), antiviral (Moukha-Chafiq *et al.*, 2006; Rashad *et al.*, 2008), anti-avian influenza virus (H5N1) (Rashad *et al.*, 2010), anti-inflammatory (Atatreh *et al.*, 2019), anti-leishmanial (Jorda *et al.*, 2011; Llanos-Cuentas *et al.*, 1997), anticancer (Chauhan & Kumar, 2013), and anti-bacterial activity (Rostamizadeh *et al.*, 2013).

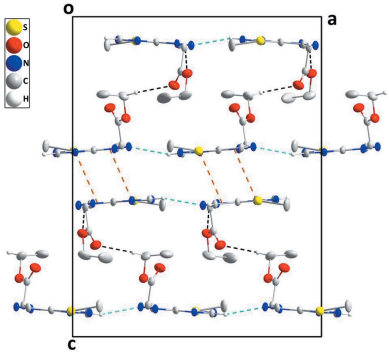

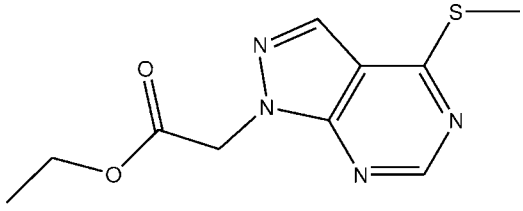

As a continuation of our research on the development of N-substituted pyrazolo[3,4-*d*]pyrimidine derivatives and the evaluation of their potential pharmacological activities, the

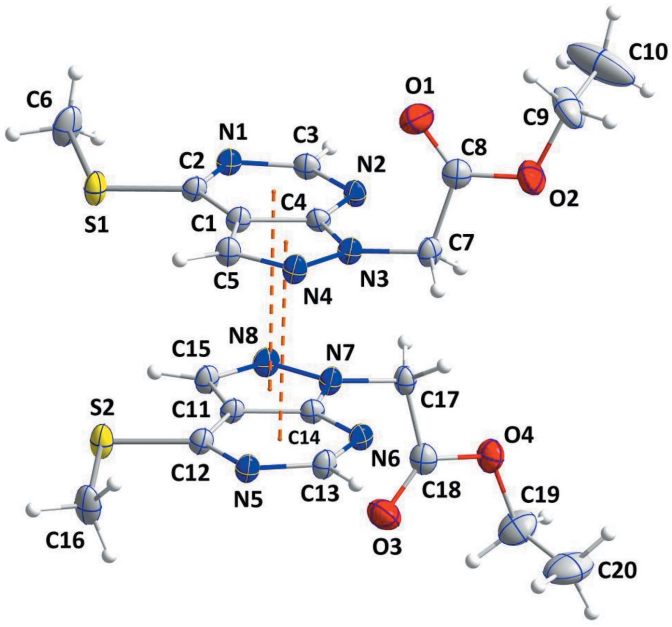

Figure 1
The asymmetric unit with the labeling scheme and displacement ellipsoids drawn at the 50% probability level. The π-stacking interactions are shown by dashed lines.

title compound, $C_{10}H_{12}N_4O_2S$, **I**, was synthesized by the reaction of ethyl 2-bromoacetate with 4-(methylsulfanyl)-1*H*-pyrazolo[3,4-*d*]pyrimidine and potassium carbonate in the presence of potassium chloride and tetra-*n*-butylammonium bromide as catalysts. We report herein the synthesis, molecular and crystal structures, Hirshfeld surface analysis, and density functional theory (DFT) computational calculations carried out at the B3LYP/6–311 G(d,p) level along with calculation of the molecular electrostatic potential (MEP) surfaces of **I**.

2. Structural commentary

The asymmetric unit of **I** contains two molecules (Fig. 1), differing slightly in the rotational orientations of the methyl groups (Fig. 2). For the molecule containing S1, the pyrazolopyrimidine moiety is planar to within 0.023 (2) Å (r.m.s. deviation = 0.0115) with N4 being the most distant atom from the mean plane. For the molecule containing S2, the bicyclic unit is planar to within 0.020 (3) Å (r.m.s. deviation = 0.0115) with C11 being the most distant atom from the mean plane. The dihedral angle between the mean planes of the bicyclic units is 2.16 (2)°.

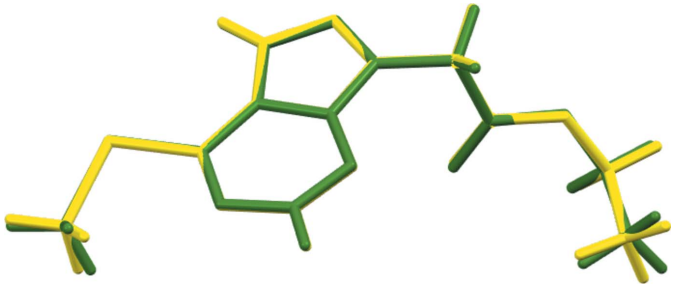

Figure 2
Overlay of the two independent molecules (yellow = molecule containing S1, green = molecule containing S2).

Table 1
Hydrogen-bond geometry (Å, °).

D—H···A	D—H	H···A	D···A	D—H···A
C3—H3···N4^{i}	0.95	2.55	3.450 (4)	158
C5—H5···O2^{ii}	0.95	2.57	3.314 (4)	136
C13—H13···N8^{iii}	0.95	2.56	3.470 (4)	159
C19—H19*A*···O1^{iv}	0.99	2.52	3.490 (5)	166

Symmetry codes: (i) $x+\frac{1}{2}, -y+\frac{3}{2}, z$; (ii) $x, y+1, z$; (iii) $x-\frac{1}{2}, -y+\frac{3}{2}, z$; (iv) $-x+\frac{3}{2}, y-\frac{1}{2}, z-\frac{1}{2}$.

3. Supramolecular features

In the crystal, chains extending parallel to the *a* axis are formed by molecules containing S1 through weak C3—H3···N4 hydrogen bonds and parallel chains by molecules containing S2 through C13—H13···N8 hydrogen bonds (Table 1). The chains containing S1 are linked into sheets parallel to the *ab* plane by C5—H5···O2 hydrogen bonds while the chains containing S2 are interspersed between these layers and connect them by C19—H19*A*···O1 hydrogen bonds. In addition, the different molecules are associated through complementary π-stacking interactions between five- and six-membered rings [centroid–centroid distance = 3.422 (2) Å; slippage 1.034 Å] (Figs. 1 and 3).

4. Hirshfeld surface analysis

In order to visualize the intermolecular interactions in the crystal of the title compound, a Hirshfeld surface (HS)

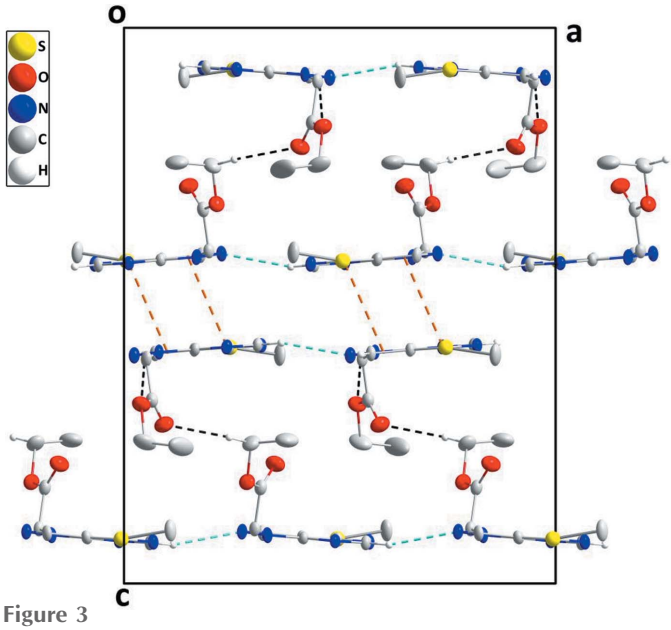

Figure 3
Packing of the molecules viewed along the *b*-axis direction with C—H···O and C—H···N hydrogen bonds shown, respectively, by black and light-blue dashed lines. The π-stacking interactions are shown by orange dashed lines.

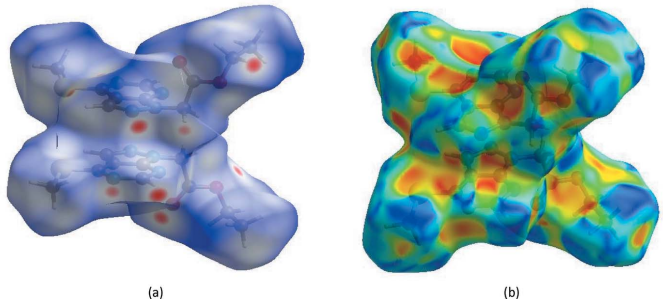

Figure 4
(*a*) View of the three-dimensional Hirshfeld surface of the title compound, plotted over d_{norm} in the range −0.7208 to 1.5611 a.u. and (*b*) Hirshfeld surface of the title compound plotted over shape-index.

analysis (Hirshfeld, 1977) was carried out by using *Crystal Explorer 17.5* (Spackman *et al.*, 2021). In the HS plotted over d_{norm} (Fig. 4*a*), the white surface indicates contacts with distances equal to the sum of van der Waals radii, and the red and blue colors indicate distances shorter or longer than the van der Waals radii, respectively (Venkatesan *et al.*, 2016). The shape-index of the HS is a tool to visualize the π–π stacking by the presence of adjacent red and blue triangles. If there are no adjacent red and/or blue triangles, then there are no π–π interactions. However, Fig. 4*b* clearly suggests that there are π–π interactions in **I**.

The overall two-dimensional fingerprint plot, Fig. 5*a*, and those delineated into H···H, H···O/O···H, H···N/N···H, H···C/C···H, H···S/S···H, N···S/S···N, C···S/S···C, O···S/S···O and O···O contacts (McKinnon *et al.*, 2007) are illustrated in Fig. 5*b–j*, respectively, together with their relative contributions to the Hirshfeld surface. The most important interaction is H···H, contributing 43.5% to the overall crystal packing, which is reflected in Fig. 5*b* as widely scattered points of high density due to the large hydrogen content of the molecule with the tip at $d_e = d_i = 1.08$ Å. The pair of the scattered points of spikes in the H···O/O···H fingerprint plot (17.9% contribution to the HS, Fig. 5*c*), has a symmetric distribution of points with the tips at $d_e + d_i = 2.40$ Å. The H···N/N···H contacts, Fig. 5*d*, contribute 17.4% to the HS, and the distribution of points also has the tips at $d_e + d_i = 2.40$ Å. The large number of H···H, H···O/O···H and H···N/N ··· H interactions suggest that van der Waals interactions play the major role in the crystal packing (Hathwar *et al.*, 2015). In the absence of C—H···π interactions, the pair of characteristic wings resulting in the fingerprint plot delineated into H···C/C···H contacts, Fig. 5*e*, the 9.5% contribution to the HS is viewed with the tips at $d_e + d_i = 2.67$ Å. The H···S/S···H contacts, Fig. 5*f*, with a 8.9% contribution to the HS are viewed with the pair of the scattered points of spikes at $d_e + d_i = 2.85$ Å. The symmetric distribution of points of the N···S/S···N contacts, Fig. 5*g*, with a 1.7% contribution to the HS appear as a pair of spikes of scattered points with the tips at $d_e + d_i = 3.33$ Å. Finally, the contributions of the remaining C···S/S···C, O···S/S···O and O···O contacts (Fig. 5*h–j*) are smaller than 1.0% to the HS with low densities of points.

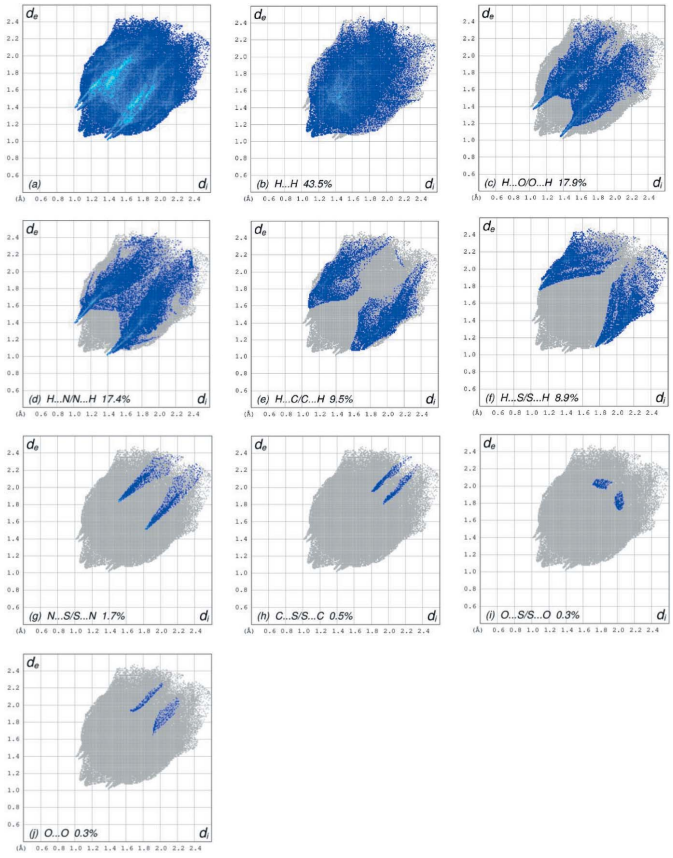

Figure 5
The full two-dimensional fingerprint plots for the title compound, showing (*a*) all interactions, and delineated into (*b*) H···H, (*c*) H···O/O···H, (*d*) H···N/N···H, (*e*) H···C/C···H, (*f*) H···S/S···H, (*g*) N···S/S···N, (*h*) C···S/S···C, (*i*) O···S/S···O and (*j*) O···O interactions. The d_i and d_e values are the closest internal and external distances (in Å) from given points on the Hirshfeld surface.

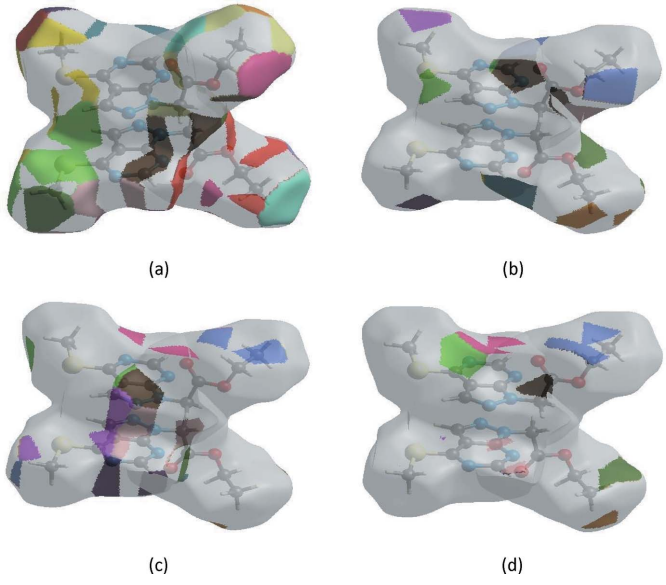

Figure 6
The Hirshfeld surface representations with the function d_{norm} plotted onto the surface for (*a*) H···H, (*b*) H···O/O···H and (*c*) H···C/C···H interactions.

Table 2
Comparison of the selected (X-ray and DFT) geometric data (Å, °).

Bonds/angles	X-ray	B3LYP/6–311G(d,p)
S1—C2	1.740 (3)	1.765
S1—C6	1.804 (3)	1.824
O1—C8	1.196 (4)	1.204
O2—C8	1.332 (4)	1.337
O2—C9	1.463 (5)	1.453
N1—C2	1.332 (3)	1.329
N1—C3	1.356 (4)	1.350
N2—C3	1.325 (4)	1.325
N2—C4	1.344 (4)	1.339
N3—C4	1.353 (4)	1.359
N3—N4	1.370 (3)	1.363
N3—C7	1.440 (4)	1.443
N4—C5	1.319 (4)	1.318
C2—S1—C6	101.68 (14)	101.324
C8—O2—C9	117.3 (3)	117.442
C2—N1—C3	117.5 (2)	117.378
C3—N2—C4	111.9 (3)	112.041
C4—N3—N4	111.2 (2)	111.358
C4—N3—C7	127.2 (3)	127.628
N4—N3—C7	120.5 (2)	120.828
C5—N4—N3	106.4 (2)	106.802
C4—C1—C2	116.0 (2)	115.050
C4—C1—C5	104.5 (2)	104.373
C2—C1—C5	139.6 (2)	140.577
N1—C2—C1	119.9 (2)	120.011
N1—C2—S1	121.86 (19)	119.923
C4—N3—N4—C5	1.9 (4)	1.710
C7—N3—N4—C5	170.6 (3)	171.115
C3—N1—C2—C1	0.9 (5)	0.715
C3—N1—C2—S1	−178.6 (3)	−179.843
C4—N2—C3—N1	0.9 (6)	0.563
C2—N1—C3—N2	−1.3 (6)	−1.149

The Hirshfeld surface representations with the function d_{norm} plotted onto the surface are shown for the H···H, H···O/O···H, H···N/N···H and H···C/C···H interactions in Fig. 6*a*–*d*, respectively.

5. DFT calculations

The structure of **I** in the gas phase was optimized by means of density functional theory (DFT) using the hybrid B3LYP method and the 6–311 G(d,p) basis-set, which is based on Becke's model (Becke, 1993). It considers a mixture of the exact (Hartree–Fock) and density functional theory exchange utilizing the B3 functional, together with the LYP correlation functional (Lee *et al.*, 1988). After obtaining the optimized molecular structure, the harmonic vibrational frequencies were calculated at the same theoretical level to confirm that the number of imaginary frequencies is zero for the stationary point. Both the structure optimization and harmonic vibrational frequency analysis of **I** were computed with the *Gaussian 09* program (Frisch *et al.*, 2009). Theoretical and experimental results related to bond lengths and angles are in good agreement and are summarized in Table 2. The DFT calculations provide some important information on the reactivity and site selectivity of the molecular framework. Numerical values for E_{HOMO} and E_{LUMO} (Fig. 7), electronegativity (χ), hardness (η), potential (μ), electrophilicity (ω) and softness (σ) are compiled in Table 3. The electron transition from the HOMO to the LUMO energy level is shown in Fig. 7. The HOMO and LUMO are localized in the plane extending from the entire ethyl 2-(4-(methylsulfanyl)-1*H*-pyrazolo[3,4-*d*]pyrimidin-1-yl)acetate system. The energy band gap [$\Delta E = E_{LUMO} - E_{HOMO}$] of the molecule is 4.84 eV, and the frontier molecular orbital energies, E_{HOMO} and E_{LUMO} are −6.55 and −1.71 eV, respectively.

Table 3
Calculated energies.

Molecular Energy (a.u.) (eV)	Compound **I**
Total Energy *TE* (eV)	−31458.99
E_{HOMO} (eV)	−6.55
E_{LUMO} (eV)	−1.71
Gap ΔE (eV)	4.84
Dipole moment, μ (Debye)	2.79
Ionization potential, I (eV)	6.55
Electron affinity, A	1.71
Electronegativity, χ	3.13
Hardness, η	2.42
Electrophilicity index, ω	3.53
Softness, σ	0.41
Fraction of electron transferred, ΔN	0.59

6. Molecular electrostatic (MEP)

Molecular electrostatic potential (MEP) surfaces can be used to predict reactive sites for electrophilic and nucleophilic attack. The calculation of MEP surfaces was carried out on the

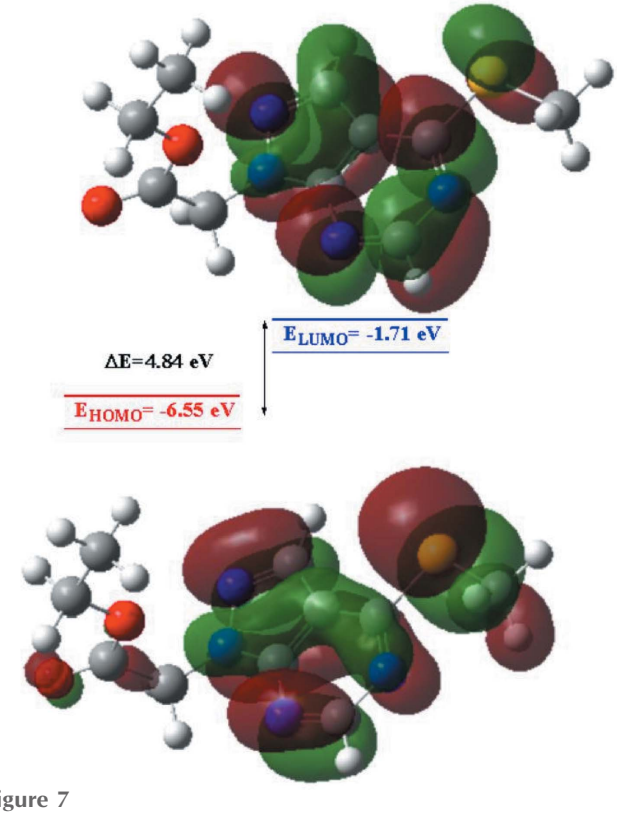

Figure 7
The energy band gap of **I**.

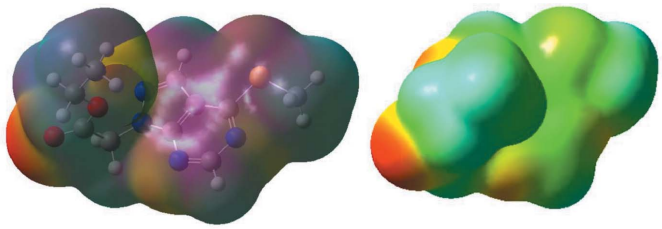

Figure 8
MEP surfaces of **I** calculated at the B3LYP/6–311 G level.

basis of B3LYP/6-31G-optimized structures using the program *Gauss View*. The total electron density onto which the electrostatic potential surface has been mapped is shown in Fig. 8. This figure provides a visual representation of the chemically active sites and comparative reactivity of atoms where the red regions denote the most negative electrostatic potential, blue represents regions with the most positive electrostatic potential, and green represents the region of zero potential. Fig. 8 confirms the existence of intermolecular C—H···O and C—H···N hydrogen-bonding interactions.

7. Database survey

A search of the Cambridge Structural Database (CSD: Groom *et al.*, 2016; updated to March 2022) with the search fragment **II** (Fig. 9) gave 18 hits of which **III** (XOVRUX; El Fal *et al.*, 2014) is the closest to **I**. All the others contain an additional methylsulfanyl substituent at the 6-position on the pyrimidine ring and a three-carbon chain attached to the nitrogen at the 1-position with various aromatic groups on the end of the chain including a second bis(methylsulfanyl)pyrazolopyrimidine moiety. These were designed to study possible intramolecular π-stacking interactions and are not considered close analogs of **I**. One other close analog is **IV** (El Hafi *et al.*, 2017). In **III**, the molecule lies on a mirror plane and so is rigorously planar. There is only one molecule in the asymmetric unit and the packing consists of head-to-tail π-stacking of the molecules along the *c* axis direction with a centroid-to-centroid distance of 3.6062 (8) Å. In **IV**, $Z' = 2$ as in **I** but the two independent molecules do not have the pyrazolopyrimidine moieties approximately parallel to one another as in **I**. Instead of chains, a self-dimer is formed by each independent molecule, and each type of dimer is π-stacked in a head-to-tail fashion, forming stepped stacks inclined by *ca* $\pm 51^\circ$ to the *bc* plane.

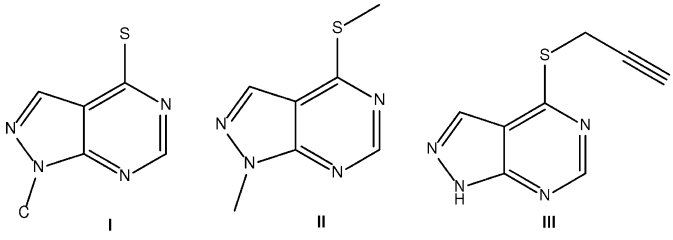

Figure 9
4-(Methylsulfanyl)-1*H*-pyrazolo[3,4-*d*]pyrimidine analogues.

Table 4
Experimental details.

Crystal data	
Chemical formula	$C_{10}H_{12}N_4O_2S$
M_r	252.30
Crystal system, space group	Orthorhombic, $Pna2_1$
Temperature (K)	150
a, *b*, *c* (Å)	15.207 (2), 7.9249 (11), 19.540 (3)
V (Å^3)	2354.9 (6)
Z	8
Radiation type	Mo $K\alpha$
μ (mm^{-1})	0.27
Crystal size (mm)	0.40 × 0.17 × 0.17
Data collection	
Diffractometer	Bruker Smart *APEX* CCD
Absorption correction	Multi-scan (*SADABS*; Krause *et al.*, 2015)
T_{min}, T_{max}	0.86, 0.96
No. of measured, independent and observed [$I > 2\sigma(I)$] reflections	43340, 6339, 5436
R_{int}	0.034
(sin $\theta/\lambda)_{max}$ (Å^{-1})	0.687
Refinement	
$R[F^2 > 2\sigma(F^2)]$, $wR(F^2)$, *S*	0.043, 0.122, 1.09
No. of reflections	6339
No. of parameters	311
No. of restraints	1
H-atom treatment	H-atom parameters constrained
$\Delta\rho_{max}$, $\Delta\rho_{min}$ (e Å^{-3})	0.57, −0.47
Absolute structure	Flack *x* determined using 2355 quotients $[(I^+)-(I^-)]/[(I^+)+(I^-)]$ (Parsons *et al.*, 2013)
Absolute structure parameter	0.08 (4)

Computer programs: *APEX3* and *SAINT* (Bruker, 2016), *SHELXT* (Sheldrick, 2015*a*), *SHELXL2018/1* (Sheldrick, 2015*b*), *DIAMOND* (Brandenburg & Putz, 2012) and *publCIF* (Westrip, 2010).

8. Synthesis and crystallization

To a solution of 4-(methylsulfanyl)-1*H*-pyrazolo[3,4-*d*]pyri-]pyrimidine (10 mmol), ethyl 2-bromoacetate (10 mmol) and potassium carbonate (6.51 mmol) in dimethylformamide (DMF; 40 ml) a catalytic amount of tetra-*n*-butylammonium bromide (0.33 mmol) was added. The mixture was stirred for 24 h. The solid material was removed by filtration and the solvent evaporated *in vacuo*. The resulting solid product was purified by recrystallization from ethanol to afford colorless crystals in 82% yield. ^{1}H NMR (300 MHz, $CDCl_3$): 1.23 (*t*, 3H, CH_3); 2.69 (*s*, 3H, CH_3); 4.20 (*q*, 2H, CH_2); 5.20 (*s*, 2H, CH_2); 8.08 (*s*,1H, H_3); 8.70 (*s*, 1H, H_6).

9. Refinement

Crystal, data collection and refinement details are given in Table 4. Although intensity statistics indicated the centrosymmetric space group *Pbca*, structure solution by direct and Patterson methods revealed serious disorder. The use of dual space methods (*SHELXT*; Sheldrick, 2015*a*) gave an ordered solution in the non-centrosymmetric space group $Pca2_1$ as the only option. The model refined smoothly and gave a reasonable value for the Flack parameter. H atoms attached to carbon were placed in calculated positions (C—H = 0.95–

0.99 Å using isotropic displacement parameters 1.2–1.5 times those of the parent atoms).

Funding information

JTM thanks Tulane University for support of the Tulane Crystallography Laboratory. TH is grateful to Hacettepe University Scientific Research Project Unit (grant No. 013 D04 602 004).

References

Atatreh, N., Youssef, A. M., Ghattas, M. A., Al Sorkhy, M., Alrawashdeh, S., Al-Harbi, K. B., El-Ashmawy, I. M., Almundarij, T. I., Abdelghani, A. A. & Abd-El-Aziz, A. S. (2019). *Bioorg. Chem.* **86**, 393–400.

Becke, A. D. (1993). *J. Chem. Phys.* **98**, 5648–5652.

Brandenburg, K. & Putz, H. (2012). *DIAMOND*. Crystal Impact GbR, Bonn, Germany.

Bruker (2016). *APEX3* and *SAINT*. Bruker AXS, Inc., Madison, Wisconsin, USA.

Chauhan, M. & Kumar, R. (2013). *Bioorg. Med. Chem.* **21**, 5657–5668.

El Fal, M., Ramli, Y., Essassi, E. M., Saadi, M. & El Ammari, L. (2014). *Acta Cryst.* E**70**, o1281.

El Hafi, M., Boulhaoua, M., Ramli, Y., Benchidmi, M., Essassi, E. M. & Mague, J. T. (2017). *IUCrData*, **2**, x171526.

Frisch, M. J., Trucks, G. W., Schlegel, H. B., Scuseria, G. E., Robb, M. A., Cheeseman, J. R., Scalmani, G., Barone, V., Mennucci, B., Petersson, G. A., Nakatsuji, H., Caricato, M., Li, X., Hratchian, H. P., Izmaylov, A. F., Bloino, J., Zheng, G., Sonnenberg, J. L., Hada, M., Ehara, M., Toyota, K., Fukuda, R., Hasegawa, J., Ishida, M., Nakajima, T., Honda, Y., Kitao, O., Nakai, H., Vreven, T., Montgomery, J. A. Jr, Peralta, J. E., Ogliaro, F., Bearpark, M., Heyd, J. J., Brothers, E., Kudin, K. N., Staroverov, V. N., Kobayashi, R., Normand, J., Raghavachari, K., Rendell, A., Burant, J. C., Iyengar, S. S., Tomasi, J., Cossi, M., Rega, N., Millam, J. M., Klene, M., Knox, J. E., Cross, J. B., Bakken, V., Adamo, C., Jaramillo, J., Gomperts, R., Stratmann, R. E., Yazyev, O., Austin, A. J., Cammi, R., Pomelli, C., Ochterski, J. W., Martin, R. L., Morokuma, K., Zakrzewski, V. G., Voth, G. A., Salvador, P., Dannenberg, J. J., Dapprich, S., Daniels, A. D., Farkas, O., Foresman, J. B., Ortiz, J. V., Cioslowski, J. & Fox, D. J. (2009). *GAUSSIAN09*. Gaussian Inc., Wallingford, CT, US

Groom, C. R., Bruno, I. J., Lightfoot, M. P. & Ward, S. C. (2016). *Acta Cryst.* B**72**, 171–179.

Hathwar, V. R., Sist, M., Jørgensen, M. R. V., Mamakhel, A. H., Wang, X., Hoffmann, C. M., Sugimoto, K., Overgaard, J. & Iversen, B. B. (2015). *IUCrJ*, **2**, 563–574.

Hirshfeld, H. L. (1977). *Theor. Chim. Acta*, **44**, 129–138.

Jorda, R., Sacerdoti-Sierra, N., Voller, J., Havlíček, L., Kráčalíková, K., Nowicki, M. W., Nasereddin, A., Kryštof, V., Strnad, M., Walkinshaw, M. D. & Jaffe, C. L. (2011). *Bioorg. Med. Chem. Lett.* **21**, 4233–4237.

Krause, L., Herbst-Irmer, R., Sheldrick, G. M. & Stalke, D. (2015). *J. Appl. Cryst.* **48**, 3–10.

Lee, C., Yang, W. & Parr, R. G. (1988). *Phys. Rev. B*, **37**, 785–789.

Llanos-Cuentas, A., Echevarria, J., Cruz, M., La Rosa, A., Campos, P., Campos, M., Franke, E., Berman, J., Modabber, F. & Marr, J. (1997). *Clin. Infect. Dis.* **25**, 677–684.

McKinnon, J. J., Jayatilaka, D. & Spackman, M. A. (2007). *Chem. Commun.* pp. 3814–3816.

Moukha-Chafiq, O., Taha, M. L., Lazrek, H. B., Vasseur, J. J. & Clercq, E. D. (2006). *Nucleosides Nucleotides Nucleic Acids*, **25**, 849–860.

Moukha-chafiq, O., Taha, M. L. & Mouna, A. (2007). *Nucleosides Nucleotides Nucleic Acids*, **26**, 1107–1110.

Parsons, S., Flack, H. D. & Wagner, T. (2013). *Acta Cryst.* B**69**, 249–259.

Rao, R. N. & Chanda, K. (2020). *Bioorg. Chem.* **99**, 103801.

Rashad, A. E., Hegab, M. I., Abdel-Megeid, R. E., Micky, J. A. & Abdel-Megeid, F. M. (2008). *Bioorg. Med. Chem.* **16**, 7102–7106.

Rashad, A. E., Shamroukh, A. H., Abdel-Megeid, R. E., Mostafa, A., Ali, M. A. & Banert, K. (2010). *Nucleosides Nucleotides Nucleic Acids*, **29**, 809–820.

Rostamizadeh, S., Nojavan, M., Aryan, R., Sadeghian, H. & Davoodnejad, M. (2013). *Chin. Chem. Lett.* **24**, 629–632.

Schenone, S., Radi, M., Musumeci, F., Brullo, C. & Botta, M. (2014). *Chem. Rev.* **114**, 7189–7238.

Sheldrick, G. M. (2015*a*). *Acta Cryst.* A**71**, 3–8.

Sheldrick, G. M. (2015*b*). *Acta Cryst.* C**71**, 3–8.

Spackman, P. R., Turner, M. J., McKinnon, J. J., Wolff, S. K., Grimwood, D. J., Jayatilaka, D. & Spackman, M. A. (2021). *J. Appl. Cryst.* **54**, 1006–1011.

Tintori, C., Fallacara, A. L., Radi, M., Zamperini, C., Dreassi, E., Crespan, E., Maga, G., Schenone, S., Musumeci, F., Brullo, C., Richters, A., Gasparrini, F., Angelucci, A., Festuccia, C., Delle Monache, S., Rauh, D. & Botta, M. (2015). *J. Med. Chem.* **58**, 347–361.

Venkatesan, P., Thamotharan, S., Ilangovan, A., Liang, H. & Sundius, T. (2016). *Spectrochim. Acta A Mol. Biomol. Spectrosc.* **153**, 625–636.

Westrip, S. P. (2010). *J. Appl. Cryst.* **43**, 920–925.

supporting information

Acta Cryst. (2022). E**78**, 1265-1270 [https://doi.org/10.1107/S2056989022011112]

Crystal structure, Hirshfeld surface analysis and DFT calculations of ethyl 2-[4-(methylsulfanyl)-1*H*-pyrazolo[3,4-*d*]pyrimidin-1-yl]acetate

Younesse Ait Elmachkouri, Ezaddine Irrou, Samira Dalbouha, Hassan Ouachtak, Joel T. Mague, Tuncer Hökelek, Lhoussaine El Ghayati, Nada Kheira Sebbar and Mohamed Labd Taha

Computing details

Data collection: *APEX3* (Bruker, 2016); cell refinement: *SAINT* (Bruker, 2016); data reduction: *SAINT* (Bruker, 2016); program(s) used to solve structure: *SHELXT* (Sheldrick, 2015*a*); program(s) used to refine structure: *SHELXL2018/1* (Sheldrick, 2015*b*); molecular graphics: *DIAMOND* (Brandenburg & Putz, 2012); software used to prepare material for publication: *publCIF* (Westrip, 2010).

Ethyl 2-[4-(methylsulfanyl)-1*H*-pyrazolo[3,4-*d*]pyrimidin-1-yl]acetate

Crystal data

$C_{10}H_{12}N_4O_2S$
M_r = 252.30
Orthorhombic, $Pna2_1$
a = 15.207 (2) Å
b = 7.9249 (11) Å
c = 19.540 (3) Å
V = 2354.9 (6) Å^3
Z = 8
$F(000)$ = 1056
D_x = 1.423 Mg m^{-3}
Mo $K\alpha$ radiation, λ = 0.71073 Å
Cell parameters from 9868 reflections
θ = 2.8–29.2°
μ = 0.27 mm^{-1}
T = 150 K
Column, colourless
0.40 × 0.17 × 0.17 mm

Data collection

Bruker Smart APEX CCD diffractometer
Radiation source: fine-focus sealed tube
Graphite monochromator
Detector resolution: 8.3333 pixels mm^{-1}
φ and ω scans
Absorption correction: multi-scan (*SADABS*; Krause *et al.*, 2015)
T_{min} = 0.86, T_{max} = 0.96
43340 measured reflections
6339 independent reflections
5436 reflections with $I > 2\sigma(I)$
R_{int} = 0.034
θ_{max} = 29.2°, θ_{min} = 2.1°
h = −20→20
k = −10→10
l = −26→26

Refinement

Refinement on F^2
Least-squares matrix: full
$R[F^2 > 2\sigma(F^2)]$ = 0.043
$wR(F^2)$ = 0.122
S = 1.09
6339 reflections
311 parameters
1 restraint
Primary atom site location: dual
Secondary atom site location: difference Fourier map
Hydrogen site location: inferred from neighbouring sites
H-atom parameters constrained
$w = 1/[\sigma^2(F_o^2) + (0.0807P)^2 + 0.1629P]$ where $P = (F_o^2 + 2F_c^2)/3$

$(\Delta/\sigma)_{max}$ = 0.001
$\Delta\rho_{max}$ = 0.57 e Å^{-3}
$\Delta\rho_{min}$ = −0.47 e Å^{-3}

Absolute structure: Flack *x* determined using 2355 quotients $[(I^+)-(I^-)]/[(I^+)+(I^-)]$ (Parsons *et al.*, 2013)
Absolute structure parameter: 0.08 (4)

Special details

Experimental. The diffraction data were obtained from 3 sets of 400 frames, each of width 0.5° in ω, collected at φ = 0.00, 90.00 and 180.00° and 2 sets of 800 frames, each of width 0.45° in φ, collected at ω = –30.00 and 210.00°. The scan time was 20 sec/frame.

Geometry. All esds (except the esd in the dihedral angle between two l.s. planes) are estimated using the full covariance matrix. The cell esds are taken into account individually in the estimation of esds in distances, angles and torsion angles; correlations between esds in cell parameters are only used when they are defined by crystal symmetry. An approximate (isotropic) treatment of cell esds is used for estimating esds involving l.s. planes.

Refinement. Refinement of F^2 against ALL reflections. The weighted R-factor wR and goodness of fit S are based on F^2, conventional R-factors R are based on F, with F set to zero for negative F^2. The threshold expression of $F^2 > 2\text{sigma}(F^2)$ is used only for calculating R-factors(gt) etc. and is not relevant to the choice of reflections for refinement. R-factors based on F^2 are statistically about twice as large as those based on F, and R- factors based on ALL data will be even larger. H-atoms attached to carbon were placed in calculated positions (C—H = 0.95 - 0.99 Å). All were included as riding contributions with isotropic displacement parameters 1.2 - 1.5 times those of the attached atoms. Although intensity statistics indicated a centric space group, solution in the centric space group by direct and Patterson methods indicated serious disorder while use of dual space methods (*SHELXT*, Sheldrick, 2015*a*) gave an ordered solution in the non-centric space group as the only option. Inspection of the resulting two independent molecules indicated slight differences in the rotational orientations of the methyl groups.

Fractional atomic coordinates and isotropic or equivalent isotropic displacement parameters (Å²)

	x	*y*	*z*	U_{iso}*/U_{eq}
S1	0.74531 (5)	1.26019 (8)	0.57534 (6)	0.0250 (2)
O1	0.59288 (18)	0.5947 (3)	0.71430 (14)	0.0419 (6)
O2	0.54002 (17)	0.3444 (3)	0.67778 (13)	0.0348 (5)
N1	0.81795 (14)	0.9505 (3)	0.57177 (13)	0.0203 (4)
N2	0.73831 (15)	0.6863 (3)	0.57468 (14)	0.0204 (5)
N3	0.58118 (17)	0.7265 (3)	0.58391 (18)	0.0197 (6)
N4	0.52384 (15)	0.8591 (3)	0.58972 (14)	0.0231 (5)
C1	0.66249 (16)	0.9581 (3)	0.57980 (16)	0.0184 (5)
C2	0.74420 (16)	1.0407 (3)	0.57571 (17)	0.0188 (5)
C3	0.8103 (2)	0.7801 (4)	0.5709 (2)	0.0212 (6)
H3	0.863935	0.719525	0.567069	0.025*
C4	0.66523 (19)	0.7812 (4)	0.57899 (19)	0.0180 (5)
C5	0.57179 (18)	0.9976 (4)	0.58628 (16)	0.0216 (6)
H5	0.548698	1.108876	0.587910	0.026*
C6	0.86041 (19)	1.3043 (5)	0.5889 (2)	0.0373 (8)
H6A	0.895983	1.226210	0.561563	0.056*
H6B	0.874605	1.290078	0.637458	0.056*
H6C	0.873159	1.420555	0.574958	0.056*
C7	0.55178 (19)	0.5563 (4)	0.59599 (17)	0.0232 (6)
H7A	0.584817	0.478246	0.565940	0.028*
H7B	0.488659	0.547292	0.584154	0.028*
C8	0.56492 (19)	0.5045 (4)	0.67034 (17)	0.0257 (6)
C9	0.5480 (4)	0.2701 (5)	0.7460 (3)	0.0477 (12)

H9A	0.542499	0.359900	0.780977	0.057*
H9B	0.499792	0.188164	0.753279	0.057*
C10	0.6321 (4)	0.1852 (10)	0.7541 (3)	0.090 (2)
H10A	0.631397	0.078866	0.728508	0.135*
H10B	0.642387	0.161832	0.802687	0.135*
H10C	0.679172	0.257702	0.736533	0.135*
S2	0.50616 (5)	1.26544 (10)	0.41974 (6)	0.0261 (3)
O3	0.64984 (17)	0.5962 (3)	0.28477 (13)	0.0395 (6)
O4	0.71465 (15)	0.3538 (3)	0.31719 (13)	0.0300 (5)
N5	0.43223 (15)	0.9564 (3)	0.42506 (13)	0.0213 (5)
N6	0.51119 (14)	0.6911 (3)	0.42374 (14)	0.0201 (5)
N7	0.66818 (17)	0.7297 (3)	0.4129 (2)	0.0209 (6)
N8	0.72609 (15)	0.8609 (3)	0.40662 (15)	0.0232 (5)
C11	0.58765 (16)	0.9615 (3)	0.41661 (15)	0.0184 (5)
C12	0.50642 (16)	1.0450 (3)	0.42037 (17)	0.0200 (5)
C13	0.4397 (2)	0.7853 (4)	0.4266 (2)	0.0213 (6)
H13	0.385810	0.725187	0.430208	0.026*
C14	0.58423 (18)	0.7855 (4)	0.41793 (19)	0.0174 (5)
C15	0.67840 (18)	1.0008 (4)	0.40924 (17)	0.0220 (6)
H15	0.701635	1.111868	0.406561	0.026*
C16	0.3923 (2)	1.3134 (4)	0.4044 (2)	0.0348 (8)
H16A	0.384436	1.436092	0.402463	0.052*
H16B	0.356391	1.267027	0.441574	0.052*
H16C	0.373922	1.263363	0.360831	0.052*
C17	0.69686 (19)	0.5584 (4)	0.40147 (17)	0.0207 (6)
H17A	0.663159	0.481025	0.431350	0.025*
H17B	0.759899	0.548007	0.413395	0.025*
C18	0.68337 (19)	0.5091 (4)	0.32713 (16)	0.0248 (6)
C19	0.7050 (3)	0.2858 (6)	0.2481 (2)	0.0409 (9)
H19A	0.756035	0.213066	0.237211	0.049*
H19B	0.703735	0.379662	0.214671	0.049*
C20	0.6230 (3)	0.1864 (8)	0.2426 (2)	0.0609 (13)
H20A	0.572189	0.262094	0.246137	0.091*
H20B	0.620777	0.103087	0.279587	0.091*
H20C	0.621549	0.128263	0.198327	0.091*

Atomic displacement parameters (Å²)

	U^{11}	U^{22}	U^{33}	U^{12}	U^{13}	U^{23}
S1	0.0147 (4)	0.0169 (3)	0.0433 (6)	−0.0013 (2)	0.0009 (4)	0.0005 (3)
O1	0.0495 (14)	0.0413 (14)	0.0348 (13)	−0.0087 (12)	−0.0086 (11)	−0.0026 (11)
O2	0.0448 (14)	0.0269 (12)	0.0328 (11)	−0.0026 (10)	0.0048 (10)	0.0066 (10)
N1	0.0137 (10)	0.0205 (11)	0.0267 (11)	−0.0007 (9)	0.0008 (8)	−0.0002 (10)
N2	0.0162 (11)	0.0167 (11)	0.0283 (12)	0.0011 (8)	−0.0018 (8)	0.0012 (12)
N3	0.0109 (11)	0.0192 (10)	0.0290 (16)	0.0011 (9)	−0.0001 (11)	−0.0014 (11)
N4	0.0156 (10)	0.0194 (12)	0.0342 (14)	0.0013 (9)	−0.0003 (9)	−0.0021 (10)
C1	0.0118 (11)	0.0186 (12)	0.0249 (12)	0.0001 (10)	0.0005 (9)	−0.0009 (11)
C2	0.0133 (11)	0.0192 (11)	0.0239 (12)	−0.0006 (10)	−0.0011 (9)	−0.0011 (12)

C3	0.0143 (13)	0.0228 (12)	0.0264 (15)	0.0022 (12)	−0.0011 (12)	0.0004 (15)
C4	0.0135 (12)	0.0188 (11)	0.0216 (14)	0.0000 (11)	−0.0012 (11)	0.0014 (14)
C5	0.0133 (13)	0.0198 (14)	0.0316 (16)	0.0005 (10)	0.0006 (11)	0.0001 (12)
C6	0.0180 (14)	0.0295 (18)	0.064 (2)	−0.0067 (13)	−0.0016 (14)	−0.0057 (16)
C7	0.0158 (13)	0.0197 (14)	0.0340 (17)	−0.0043 (11)	−0.0011 (11)	0.0016 (12)
C8	0.0196 (14)	0.0269 (15)	0.0305 (14)	0.0007 (11)	0.0017 (11)	−0.0002 (11)
C9	0.070 (3)	0.036 (2)	0.036 (2)	0.009 (2)	0.015 (2)	0.0150 (17)
C10	0.086 (4)	0.136 (5)	0.048 (3)	0.075 (4)	0.008 (3)	0.024 (3)
S2	0.0150 (4)	0.0169 (4)	0.0464 (7)	0.0009 (2)	0.0005 (4)	−0.0014 (4)
O3	0.0493 (14)	0.0362 (13)	0.0329 (12)	0.0118 (12)	−0.0063 (11)	0.0024 (10)
O4	0.0330 (11)	0.0229 (11)	0.0341 (11)	0.0074 (9)	0.0022 (9)	−0.0045 (9)
N5	0.0146 (10)	0.0183 (11)	0.0310 (12)	0.0003 (9)	−0.0015 (9)	−0.0011 (10)
N6	0.0145 (10)	0.0201 (12)	0.0258 (12)	−0.0028 (9)	0.0001 (8)	0.0012 (11)
N7	0.0135 (12)	0.0165 (11)	0.0326 (17)	0.0007 (9)	−0.0013 (12)	−0.0025 (11)
N8	0.0138 (10)	0.0239 (13)	0.0318 (13)	−0.0030 (9)	0.0014 (9)	0.0005 (11)
C11	0.0128 (11)	0.0185 (12)	0.0240 (12)	−0.0008 (10)	−0.0015 (9)	−0.0010 (11)
C12	0.0165 (12)	0.0182 (12)	0.0252 (12)	0.0001 (10)	0.0000 (9)	−0.0019 (13)
C13	0.0149 (13)	0.0196 (12)	0.0293 (16)	−0.0023 (12)	0.0011 (12)	−0.0007 (15)
C14	0.0127 (12)	0.0184 (11)	0.0211 (14)	−0.0002 (11)	0.0005 (10)	0.0004 (14)
C15	0.0137 (12)	0.0195 (14)	0.0328 (17)	−0.0035 (10)	−0.0020 (11)	0.0012 (12)
C16	0.0188 (14)	0.0225 (17)	0.063 (2)	0.0052 (12)	−0.0030 (14)	0.0021 (15)
C17	0.0160 (13)	0.0160 (13)	0.0299 (15)	0.0021 (11)	0.0005 (11)	0.0006 (12)
C18	0.0189 (13)	0.0234 (15)	0.0321 (15)	0.0017 (11)	0.0022 (11)	−0.0006 (12)
C19	0.043 (2)	0.047 (2)	0.033 (2)	0.0027 (19)	0.0083 (18)	−0.0131 (19)
C20	0.073 (3)	0.082 (3)	0.028 (2)	−0.012 (3)	−0.003 (2)	−0.007 (2)

Geometric parameters (Å, º)

S1—C2	1.740 (3)	S2—C12	1.747 (3)
S1—C6	1.804 (3)	S2—C16	1.798 (3)
O1—C8	1.196 (4)	O3—C18	1.192 (4)
O2—C8	1.332 (4)	O4—C18	1.334 (3)
O2—C9	1.463 (5)	O4—C19	1.461 (5)
N1—C2	1.332 (3)	N5—C12	1.332 (3)
N1—C3	1.356 (4)	N5—C13	1.361 (4)
N2—C3	1.325 (4)	N6—C13	1.320 (4)
N2—C4	1.344 (4)	N6—C14	1.344 (4)
N3—C4	1.353 (4)	N7—C14	1.355 (4)
N3—N4	1.370 (3)	N7—N8	1.368 (3)
N3—C7	1.440 (4)	N7—C17	1.443 (4)
N4—C5	1.319 (4)	N8—C15	1.326 (4)
C1—C4	1.403 (4)	C11—C14	1.396 (4)
C1—C2	1.406 (3)	C11—C12	1.403 (3)
C1—C5	1.420 (4)	C11—C15	1.422 (4)
C3—H3	0.9500	C13—H13	0.9500
C5—H5	0.9500	C15—H15	0.9500
C6—H6A	0.9800	C16—H16A	0.9800
C6—H6B	0.9800	C16—H16B	0.9800

C6—H6C	0.9800	C16—H16C	0.9800
C7—C8	1.523 (4)	C17—C18	1.518 (4)
C7—H7A	0.9900	C17—H17A	0.9900
C7—H7B	0.9900	C17—H17B	0.9900
C9—C10	1.453 (6)	C19—C20	1.480 (6)
C9—H9A	0.9900	C19—H19A	0.9900
C9—H9B	0.9900	C19—H19B	0.9900
C10—H10A	0.9800	C20—H20A	0.9800
C10—H10B	0.9800	C20—H20B	0.9800
C10—H10C	0.9800	C20—H20C	0.9800

C2—S1—C6	101.68 (14)	C12—S2—C16	102.41 (14)
C8—O2—C9	117.3 (3)	C18—O4—C19	116.0 (3)
C2—N1—C3	117.5 (2)	C12—N5—C13	117.1 (2)
C3—N2—C4	111.9 (3)	C13—N6—C14	111.7 (3)
C4—N3—N4	111.2 (2)	C14—N7—N8	111.4 (2)
C4—N3—C7	127.2 (3)	C14—N7—C17	127.1 (3)
N4—N3—C7	120.5 (2)	N8—N7—C17	120.4 (2)
C5—N4—N3	106.4 (2)	C15—N8—N7	106.3 (2)
C4—C1—C2	116.0 (2)	C14—C11—C12	115.9 (2)
C4—C1—C5	104.5 (2)	C14—C11—C15	104.9 (2)
C2—C1—C5	139.6 (2)	C12—C11—C15	139.2 (2)
N1—C2—C1	119.9 (2)	N5—C12—C11	120.1 (2)
N1—C2—S1	121.86 (19)	N5—C12—S2	121.70 (19)
C1—C2—S1	118.28 (19)	C11—C12—S2	118.22 (19)
N2—C3—N1	129.0 (3)	N6—C13—N5	129.1 (3)
N2—C3—H3	115.5	N6—C13—H13	115.5
N1—C3—H3	115.5	N5—C13—H13	115.5
N2—C4—N3	127.3 (3)	N6—C14—N7	127.1 (3)
N2—C4—C1	125.7 (3)	N6—C14—C11	126.0 (3)
N3—C4—C1	106.9 (2)	N7—C14—C11	106.8 (2)
N4—C5—C1	111.0 (2)	N8—C15—C11	110.6 (2)
N4—C5—H5	124.5	N8—C15—H15	124.7
C1—C5—H5	124.5	C11—C15—H15	124.7
S1—C6—H6A	109.5	S2—C16—H16A	109.5
S1—C6—H6B	109.5	S2—C16—H16B	109.5
H6A—C6—H6B	109.5	H16A—C16—H16B	109.5
S1—C6—H6C	109.5	S2—C16—H16C	109.5
H6A—C6—H6C	109.5	H16A—C16—H16C	109.5
H6B—C6—H6C	109.5	H16B—C16—H16C	109.5
N3—C7—C8	111.6 (3)	N7—C17—C18	110.5 (3)
N3—C7—H7A	109.3	N7—C17—H17A	109.6
C8—C7—H7A	109.3	C18—C17—H17A	109.6
N3—C7—H7B	109.3	N7—C17—H17B	109.6
C8—C7—H7B	109.3	C18—C17—H17B	109.6
H7A—C7—H7B	108.0	H17A—C17—H17B	108.1
O1—C8—O2	126.3 (3)	O3—C18—O4	125.8 (3)
O1—C8—C7	124.8 (3)	O3—C18—C17	125.0 (3)

O2—C8—C7	108.9 (3)	O4—C18—C17	109.2 (3)
C10—C9—O2	111.0 (4)	O4—C19—C20	110.4 (3)
C10—C9—H9A	109.4	O4—C19—H19A	109.6
O2—C9—H9A	109.4	C20—C19—H19A	109.6
C10—C9—H9B	109.4	O4—C19—H19B	109.6
O2—C9—H9B	109.4	C20—C19—H19B	109.6
H9A—C9—H9B	108.0	H19A—C19—H19B	108.1
C9—C10—H10A	109.5	C19—C20—H20A	109.5
C9—C10—H10B	109.5	C19—C20—H20B	109.5
H10A—C10—H10B	109.5	H20A—C20—H20B	109.5
C9—C10—H10C	109.5	C19—C20—H20C	109.5
H10A—C10—H10C	109.5	H20A—C20—H20C	109.5
H10B—C10—H10C	109.5	H20B—C20—H20C	109.5

C4—N3—N4—C5	1.9 (4)	C14—N7—N8—C15	1.4 (5)
C7—N3—N4—C5	170.6 (3)	C17—N7—N8—C15	170.3 (3)
C3—N1—C2—C1	0.9 (5)	C13—N5—C12—C11	0.6 (5)
C3—N1—C2—S1	−178.6 (3)	C13—N5—C12—S2	−178.6 (3)
C4—C1—C2—N1	−0.4 (4)	C14—C11—C12—N5	0.2 (5)
C5—C1—C2—N1	177.9 (3)	C15—C11—C12—N5	177.4 (3)
C4—C1—C2—S1	179.2 (3)	C14—C11—C12—S2	179.4 (3)
C5—C1—C2—S1	−2.6 (6)	C15—C11—C12—S2	−3.4 (6)
C6—S1—C2—N1	−12.7 (3)	C16—S2—C12—N5	−14.1 (3)
C6—S1—C2—C1	167.8 (3)	C16—S2—C12—C11	166.6 (3)
C4—N2—C3—N1	0.9 (6)	C14—N6—C13—N5	−0.7 (6)
C2—N1—C3—N2	−1.3 (6)	C12—N5—C13—N6	−0.3 (5)
C3—N2—C4—N3	−179.6 (4)	C13—N6—C14—N7	−179.2 (4)
C3—N2—C4—C1	−0.2 (5)	C13—N6—C14—C11	1.6 (5)
N4—N3—C4—N2	177.9 (3)	N8—N7—C14—N6	179.0 (3)
C7—N3—C4—N2	10.2 (7)	C17—N7—C14—N6	11.1 (7)
N4—N3—C4—C1	−1.6 (5)	N8—N7—C14—C11	−1.6 (5)
C7—N3—C4—C1	−169.3 (3)	C17—N7—C14—C11	−169.5 (3)
C2—C1—C4—N2	0.0 (5)	C12—C11—C14—N6	−1.4 (5)
C5—C1—C4—N2	−178.8 (3)	C15—C11—C14—N6	−179.5 (3)
C2—C1—C4—N3	179.5 (3)	C12—C11—C14—N7	179.2 (3)
C5—C1—C4—N3	0.7 (4)	C15—C11—C14—N7	1.1 (4)
N3—N4—C5—C1	−1.5 (4)	N7—N8—C15—C11	−0.7 (4)
C4—C1—C5—N4	0.5 (4)	C14—C11—C15—N8	−0.3 (4)
C2—C1—C5—N4	−177.9 (4)	C12—C11—C15—N8	−177.7 (4)
C4—N3—C7—C8	74.9 (5)	C14—N7—C17—C18	75.6 (5)
N4—N3—C7—C8	−91.8 (4)	N8—N7—C17—C18	−91.4 (4)
C9—O2—C8—O1	−0.5 (5)	C19—O4—C18—O3	−1.0 (5)
C9—O2—C8—C7	179.7 (3)	C19—O4—C18—C17	178.8 (3)
N3—C7—C8—O1	2.7 (4)	N7—C17—C18—O3	−3.4 (4)
N3—C7—C8—O2	−177.5 (2)	N7—C17—C18—O4	176.7 (2)
C8—O2—C9—C10	−92.6 (5)	C18—O4—C19—C20	−93.3 (4)

Hydrogen-bond geometry (Å, º)

D—H···*A*	*D*—H	H···*A*	*D*···*A*	*D*—H···*A*
C3—H3···N4^{i}	0.95	2.55	3.450 (4)	158
C5—H5···O2^{ii}	0.95	2.57	3.314 (4)	136
C13—H13···N8^{iii}	0.95	2.56	3.470 (4)	159
C19—H19*A*···O1^{iv}	0.99	2.52	3.490 (5)	166

Symmetry codes: (i) *x*+1/2, −*y*+3/2, *z*; (ii) *x*, *y*+1, *z*; (iii) *x*−1/2, −*y*+3/2, *z*; (iv) −*x*+3/2, *y*−1/2, *z*−1/2.